

ELECTRONIC STRUCTURE AND AROMATICITY OF [12]INFINITENE. A DFT STUDY

Sladana Đorđević¹, Dušan Čočić*¹, Muntadar A. H. Al-Yassiri²,
Slavko Radenković¹, Ralph Puchta*^{3,4,5,6}

¹ *University of Kragujevac, Faculty of Science, Department of Chemistry,
Radoja Domanovića 12, P. O. Box 60, 34000 Kragujevac, Serbia*

² *University of Baghdad, College of Science, Department of Chemistry,
Al-Jadiryia, Baghdad Iraq*

³ *Fakultät Angewandte Mathematik, Physik und Allgemeinwissenschaften, Technische
Hochschule Nürnberg Georg Simon Ohm, Keßlerplatz 12, 90489 Nürnberg, Germany*

⁴ *Inorganic Chemistry, Department of Chemistry and Pharmacy,*

University of Erlangen-Nuremberg, Egerlandstr. 1, 91058 Erlangen, Germany

⁵ *Central Institute for Scientific Computing (CISC), University of Erlangen-Nuremberg,
Martensstr. 5a, 91058 Erlangen, Germany*

⁶ *Computer Chemistry Center, Department of Chemistry and Pharmacy,
University of Erlangen-Nuremberg, Nögelsbachstr. 25, 91052 Erlangen, Germany*

*Corresponding author; E-mail: dusan.cocic@pmf.kg.ac.rs, ralph.puchta@fau.de

(Received April 11, 2023; Accepted May 05, 2023)

ABSTRACT. The electronic structure and aromaticity of the [12]infinite molecule (**1**) and its formation via the Mallory reaction were studied using density functional theory (DFT). The examined reaction is based on a stepwise cyclization process. The nucleus-independent chemical shifts (NICS) were used to assess the aromatic character of the chemical species involved in the examined reactions. In addition, NICS-Scan, 2D and 3D multidimensional *off*-nucleus $\sigma_{\text{iso}}(r)$ magnetic shielding scans were also employed to examine the aromaticity of **1**. It was found that the formation of **1** is an endothermic process, as a result of the opposed stabilizing effects of aromaticity and destabilizing effects of planarity distortions found in molecules included in the considered reaction.

Keywords: NICS, infinite, reaction mechanism, DFT, aromaticity.

INTRODUCTION

Polycyclic aromatic hydrocarbons (PAHs) have been the subject of interest of chemists for more than a century (RANDIĆ, 2003). PAHs find applications in many diverse fields, such as materials (BENDIKOV *et al.* 2004), nanoscience (ANTHONY, 2006), theoretical organic chemistry (RANDIĆ, 2003; GUTMAN *et al.* 2011; REDŽEPOVIĆ *et al.* 2019) and astrochemistry (WEISMAN *et al.* 2003). Yet, these compounds can be extremely hazardous environmental pollutants usually generated during incomplete combustion of hydrocarbon-containing fuel sources (OTERO-LOBATO *et al.* 2005). Since the first experimental realization of graphene in

2004 (NOVOSELOV *et al.* 2004), extended PAHs have been attracting renewed attention (NARITA *et al.* 2015). In recent years, there has been increasing interest in non-planar aromatic structures, which are characterized with substantial steric strain while maintaining a significant extent of π -electron delocalization. Such systems include helicenes, twistacenes and Möbius aromatics (NAULET *et al.* 2018). A continuous development of synthetic chemistry enabled the production of many non-planar PAHs adopting various topologies such as cycloarenes (HOU *et al.* 2020), circulenes (MILLER *et al.* 2014), and carbon nanobelts (XIA *et al.* 2021). Recently, KRZESZEWSKI *et al.* (2022) reported the synthesis of an infinity-shaped PAH molecule (**1**) with twelve six-membered rings. The molecular structure of **1** can formally be obtained by fusing a [6]helicene with its chiral counterpart at their terminal rings (Figure 1). In addition, the infinitene **1** can be also seen as being produced by joining two cleaved coronene subunits.

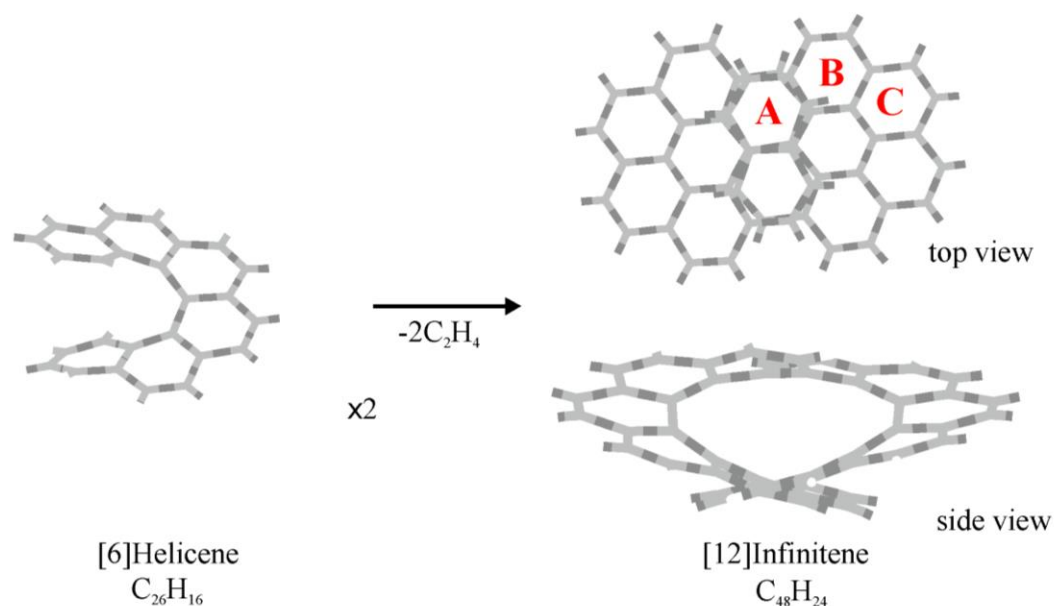


Figure 1. An imaginary “fusion” of two [6]helicene units resulting in an infinity-shaped structure of [12]infinitene (**1**).

The infinitene molecule **1** can be viewed as a member of much broader family PAHs having helically twisted structure resembling that of the infinity symbol (∞). Even at first glance, **1** looks to be a truly fascinating molecule, in particular concerning the nature of its aromaticity. The aromaticity of this molecules has been studied in two recent papers (MONACO *et al.* 2022; OROZCO-IC *et al.* 2022), and further compared with circulenes, and nanobelts (ANJALIKRISHNA *et al.* 2023). Both of these works have agreed that molecule **1** exhibits two disjointed global diatropic (aromatic) current pathways along the edges formed by 24 carbon atoms, and these current density flows never cross.

In this paper we further analyze these fascinating geometrical and aromatic features of the infinitene molecule **1**. In particular, we provide a detailed theoretical description of the synthesis reaction of **1**, by analyzing the influence of aromaticity of all chemical species involved in the reaction pathway. The aromaticity of the studied molecules was assessed by means of the nucleus independent chemical shifts (NICS) (SCHLEYER *et al.* 1996; SCHLEYER *et al.* 1997; CHEN *et al.* 2005; PUCHTA *et al.* 2022), and NICS-Scan (STANGER, 2006). Moreover, multidimensional (2D-3D) magnetic shielding contour maps were also involved in this work to detail the aromaticity of **1**. The NICS index is among the most popular aromaticity indices (GERSHONI-PORANNE and STANGER, 2015; PUCHTA *et al.* 2022).

COMPUTATIONAL METHODS

The geometry optimizations were performed using the B3LYP (LEE *et al.* 1988; BECKE 1993; STEPHENS *et al.* 1994) theory level extended by Grimme's dispersion correction (GRIMME *et al.* 2010) in combination with the 6-311+g(d,p) basis set. The obtained structures of the investigated species were characterized as minima by examining the vibrational frequencies calculated at the same theory level. The GAUSSIAN suite of programs was used for this purpose (FRISCH *et al.* 2010).

Originally, the NICS was defined as the negative value of the isotropic shielding constant calculated at the ring centre. In the recent paper (DOBROWOLSKI and LIPÍŃSKI 2016), it has been pointed out that for non-planar rings the NICS should be calculated separately, 1 Å above (NICS(1)) and 1 Å below the ring centre (NICS(-1)). As a good probe of aromaticity in non-planar molecular systems, the NICS(1)_{av} has been suggested:

$$\text{NICS}(1)_{\text{av}} = [\text{NICS}(-1) + \text{NICS}(1)]/2$$

NICS indices were calculated at B3LYP/6-311+g(d,p) level of theory.

We additionally utilized the NICS-Scan approach (STANGER 2006) for scanning multiple points as a 1D grid contains 301 ghost atoms (Bqs). The 1D lines were placed perpendicular to rings A, B, and C of [12]infinifene and extended from the rings' centers to +2/-2 Å above/below the center. Moreover, 2D and 3D grids of Bqs were also employed to obtain 2D magnetic shielding maps and 3D isotropic magnetic isosurfaces for [12]infinifene.

The planarity distortion of the hexagonal rings in the studied molecules was quantified by means of the T index (DOBROWOLSKI and LIPÍŃSKI 2016), which is defined as the root mean square deviation of all dihedral angles:

$$T = \sqrt{\frac{1}{n} \sum_{i=1}^n (\tau_{\text{CCCC}}^i)^2} \quad (1)$$

where summation goes over all n different CCCC dihedral angles (τ) in the given ring.

RESULTS AND DISCUSSION

As mentioned in the Introduction section, the aromatic character of **1** has been previously explored by means of the induced current density analyses (MONACO *et al.* 2022; OROZCO-IC *et al.* 2022). Here, we calculated the NICS values for symmetry-unique rings of **1** (Table 1). Both NICS(0) and NICS(1)_{av} reveal aromatic nature of the hexagonal rings in **1**, in line with predictions of the current-density-based analysis. The calculated T-index values (Table 1 and Figure 2) shows that all rings in **1** exhibit a significant deviation from planarity. Molecular planarity is one of the most recognized manifestations of aromaticity (KRYGOWSKI *et al.* 2014). However, it has been shown that the molecular aromaticity can survive despite very strong planarity distortions (FEIXAS *et al.* 2007). It was found that in **1** the extent of the planarity deviation of the hexagonal rings does not fully follow the change in NICS values. Yet, it is evident the infinifene molecule **1** is characterized with a substantial extent of cyclic π electron delocalization regardless of its very crude planarity distortion.

To obtain more magnetic details about **1**, Figures 3–6 show NICS-Scan and 2D-3D *off*-nucleus isotropic magnetic results for [12]infinifene. Accordingly, NICS-Scan curves (Figure 3) indicate more negative NICS for ring A, followed by B and C. Also, for each of the

rings, it is worth noticing the maximum negative NICS values are located at heights 1 Å above and below the centers of these rings. This allows assuming that the π -electron delocalization at p_z orbital regions at these heights causes such high NICS responses. Therefore, these curves elucidate magnetic behaviors like those aromatic rings.

Table 1. Calculated NICS(0) and NICS(1)_{av} values for symmetry-unique rings in **1**, as shown in Figure 1.

Ring	NICS(0)	NICS(1) _{av}	T (in degrees)
A	-7.33	-10.47	97.2
B	-6.93	-9.38	27.7
C	-5.36	-7.92	101.0

In agreement, the same shielding arrangements obtained by NICS-Scan can also be seen via Figure 4, which displays almost three identical shielding maps with minor differences at the ring centers of [12]infinifene. There are many common points between the shielding maps of [12]infinifene rings and that of benzene. For example, the central regions of the rings are dominated by magnetic shielding (blue color), the shielding cloud about C-C bonds, and the deshielded spheres (red color) surrounding carbon atoms all show similar shielding patterns to those aromatic rings.

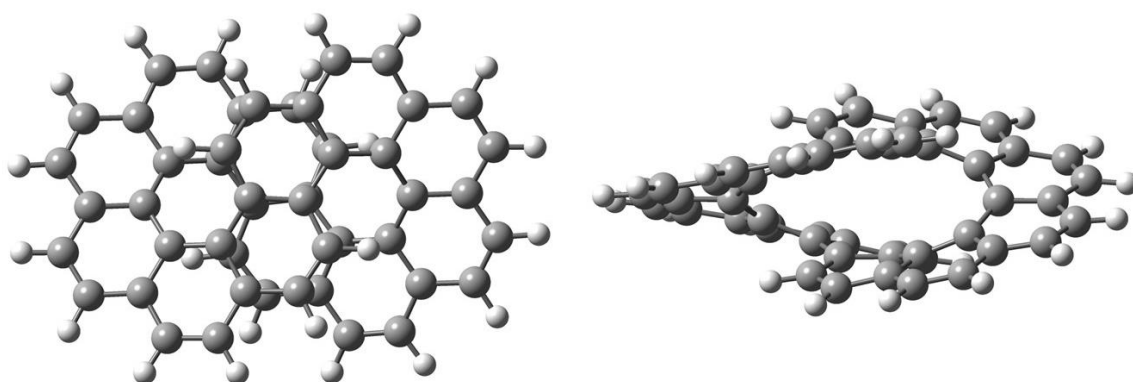


Figure 2. The B3LYP-GD3/6-311+g(d,p) optimized structure of [12]infinifene (**1**): top-view (left) and side-view (right).

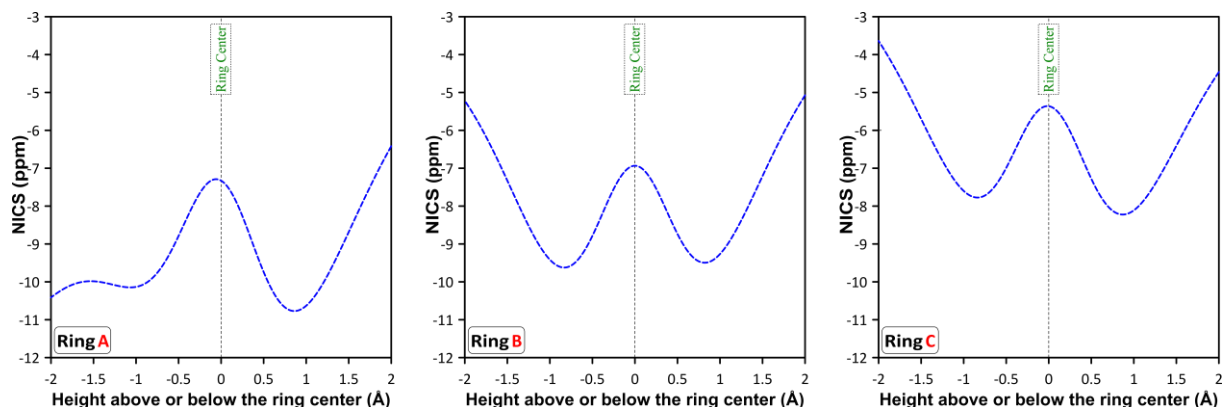


Figure 3. NICS-Scan curves calculated at the B3LYP-GIAO/6-311+G(d,p) level of theory, and scanned the magnetic shielding along a line of 301 Bq points extended from -2 Å (below) to +2 Å (above) the centers of rings A, B, and C of [12]infinifene (**1**).

As Figure 5 shows, both the grids oriented through XZ and YZ directions, maps (a) and (b), produced magnetic shielding maps of very extended shielding activity along the Z coordinate, i.e., there is a vertical expansion of the shielding up to ± 8 Å above and below the infinite rings loop. However, the two deshielded cyclones (red) at the fjord bays inside the two rings loop in maps (a) and (c) are a consequence of the induced magnetic lines at these regions that are directed against the direction of the magnetic shielding lines.

Understanding the magnetic shielding can also be achieved through the 3D isotropic magnetic isosurfaces (Figure 6). We selected three isosurfaces, red, blue, and pink which visualize the shielding values of -3, +21, and +6 (ppm), respectively. The blue isosurface precisely displays how the shielding cloud covers all the hexagonal rings skeleton of [12]infinite, indicating adequate magnetic shielding caused by the C-C bonds and electron delocalization. Also, the pink isosurface shows the shielding expansion mentioned above. Both deshielded cyclones and deshielded spheres are observable via the red isosurface.

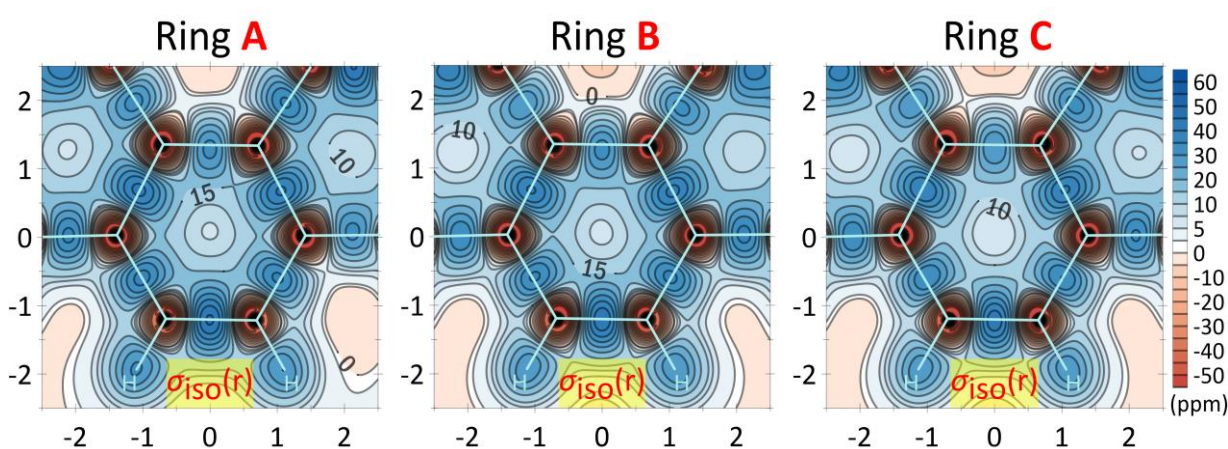


Figure 4. Isotropic magnetic shielding $\sigma_{\text{iso}}(r)$ maps calculated at the B3LYP-GIAO/6-311+G(d,p) level of theory and probed from the nuclei levels of rings A, B, and C of [12]infinite (**1**).

In this report we also aim to establish the influence of aromaticity on the reaction pathway. In particular, we are interested to see how the aromaticity with its stabilization/destabilization effects can affect the ground state of chemical species formed during the reaction process of the synthesis of **1**. For this purpose, here we examined the formation of **1** by Mallory reaction (JØRGENSEN, 2010). Our theoretical model of the reaction is stripped off any additional reagents which may be involved in the reaction, which is a common practice in this kind of theoretical assessment (REDŽEPOVIĆ *et al.* 2017; TOŠOVIĆ 2017).

Mallory reaction in itself is a photochemical-cyclization–elimination reaction where under UV irradiation, stilbene and its derivatives undergo intramolecular cyclization to form dihydrophenanthrenes (JØRGENSEN, 2010). In the presence of an oxidant, the dihydrophenanthrenes aromatize to give polycyclic aromatics. A schematic presentation of the investigated reaction is presented in Figure 7 together with the calculated relative energies (for the sake of clarity, in Figure 7 one part containing both reaction centers of the molecule is presented, while the whole structures of some molecules are presented in Figures 2 and 8).

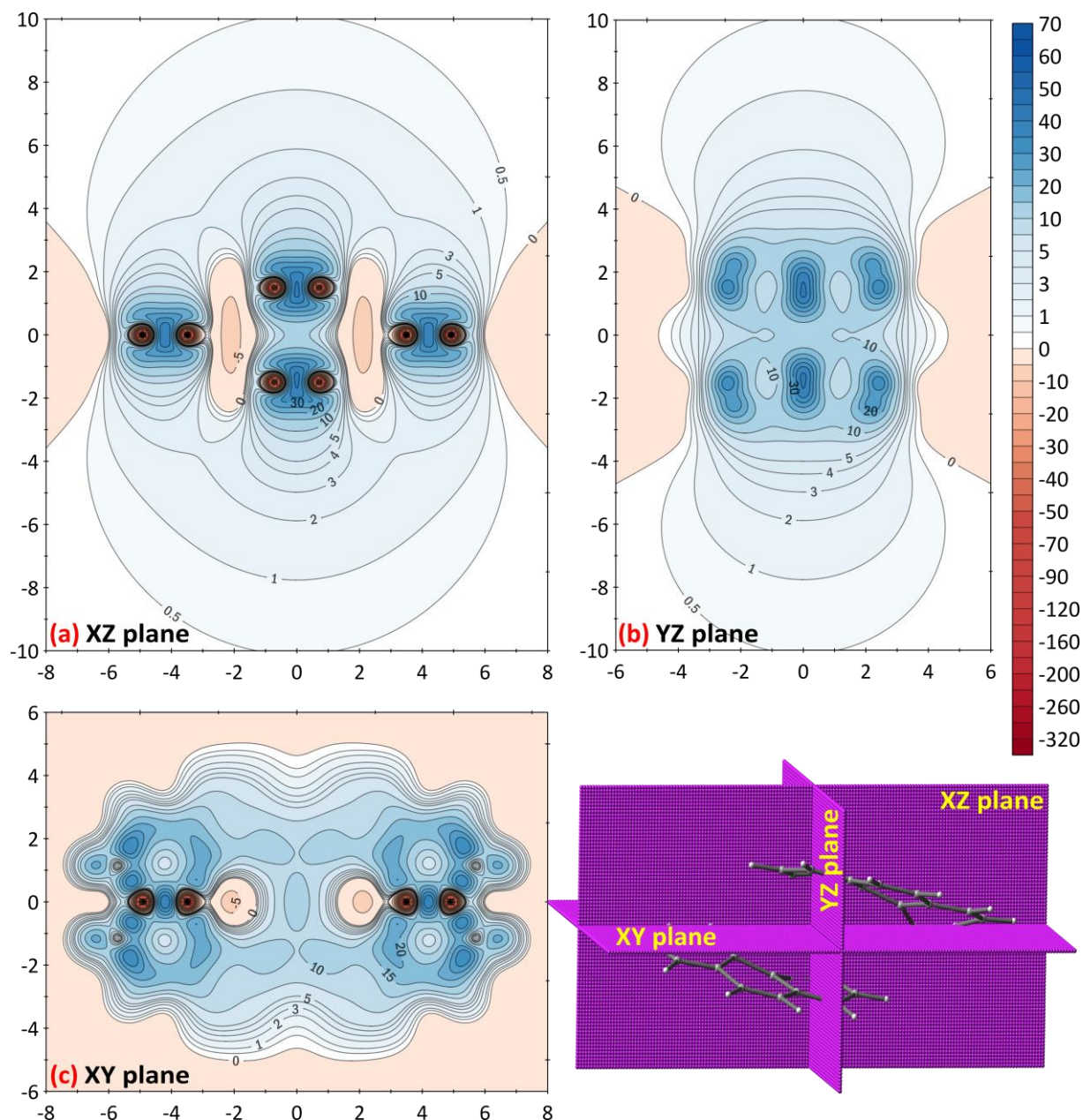


Figure 5. 2D magnetic shielding contour maps (in ppm) of [12]infinitecane (**1**) calculated at the B3LYP-GIAO/6-311+G(d,p) level of theory. The vertical maps (a) and (b) were recorded by 2D (XZ) and (YZ) grids of Bqs, respectively, while (c) is the horizontal map scanned by a 2D (XY) grid.

As mentioned above, none of the reagents which are used during the experimental realization of this kind of reaction was considered in the presented model. Additionally, all species shown in Figure 7 were characterized as local minima, so from that point of view, further on we are discussing the overall thermostability of the different species formed during the presented reaction path. The reaction starts from cyclophadien (**R**) whose optimized geometry is displayed in Figure 8. The energies of all molecules in Figure 7 are given relative to the starting cyclophadien molecule **R** (for which the relative energy equals 0 kcal/mol). The NICS indices were calculated for some of the selected species involved in the reaction depicted in Figure 7. According to the NICS values all rings in **R** exhibit a significant aromatic character (Figure 9). The first reaction step is a cyclization process which yields a product with 34.27 kcal/mol higher energy than the starting cyclophadien reactant **R**. It can be observed that the obtained intermediate **I**₁ suffers from aromaticity lost in the two rings

adjacent to the newly formed hexagonal ring, which is also found to be nonaromatic. The increased destabilization of **I**₁ relative to **R** arises as a combination of the aromaticity loss and strain magnification.

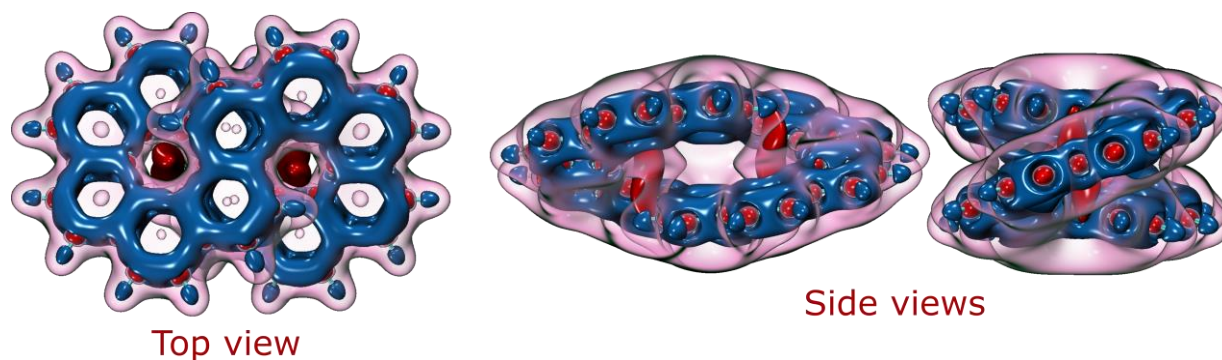


Figure 6. 3D magnetic shielding isosurfaces of [12]infinite (**1**) calculated at the B3LYP-GIAO/6-311+G(d,p) level of theory, the color/shielding value (in ppm) are red/-3, blue/+21, pink/+6.

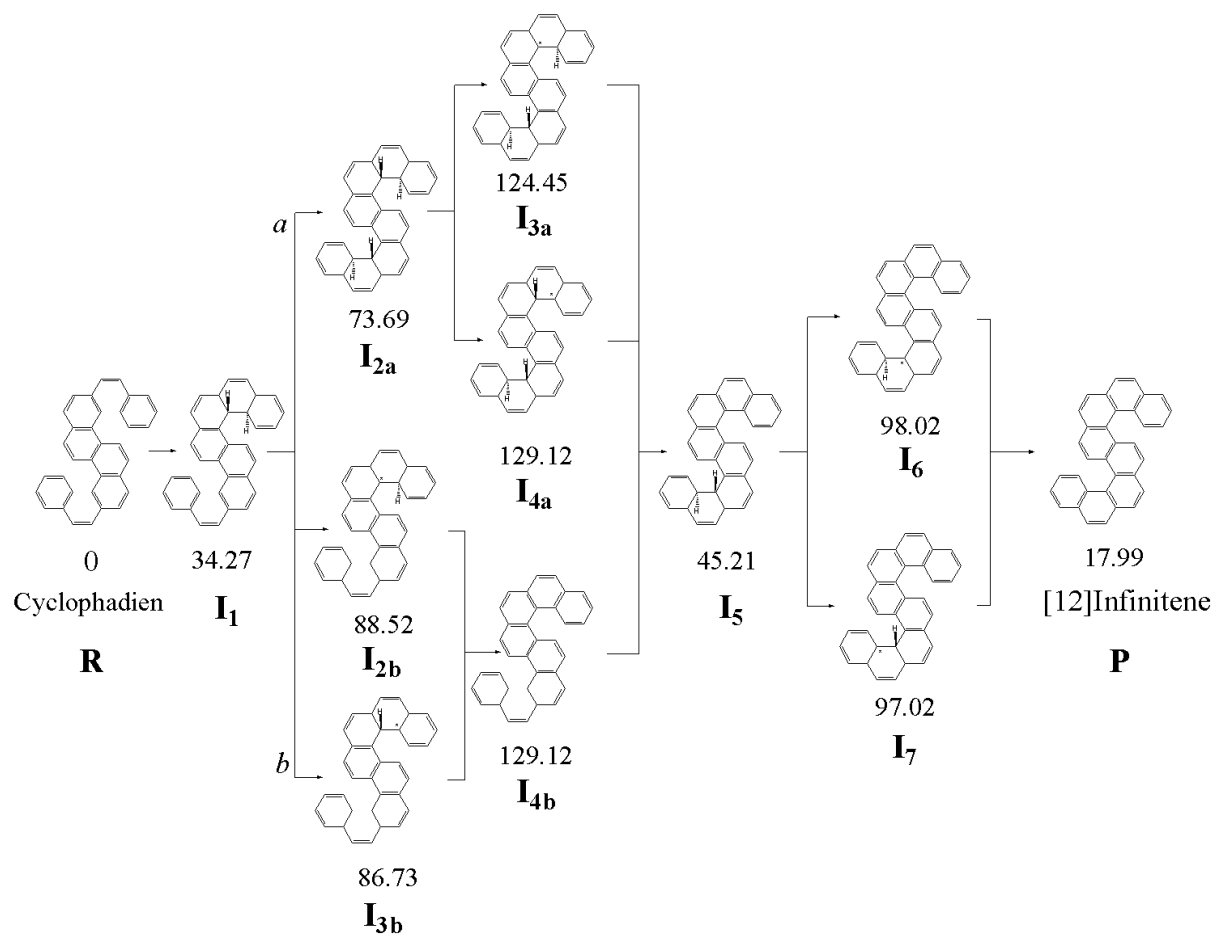


Figure 7. Schematic presentation for investigated formation reaction of [12]infinite together with calculated B3LYP-GD3/6-311+g(d,p) relative energies in kcal/mol.

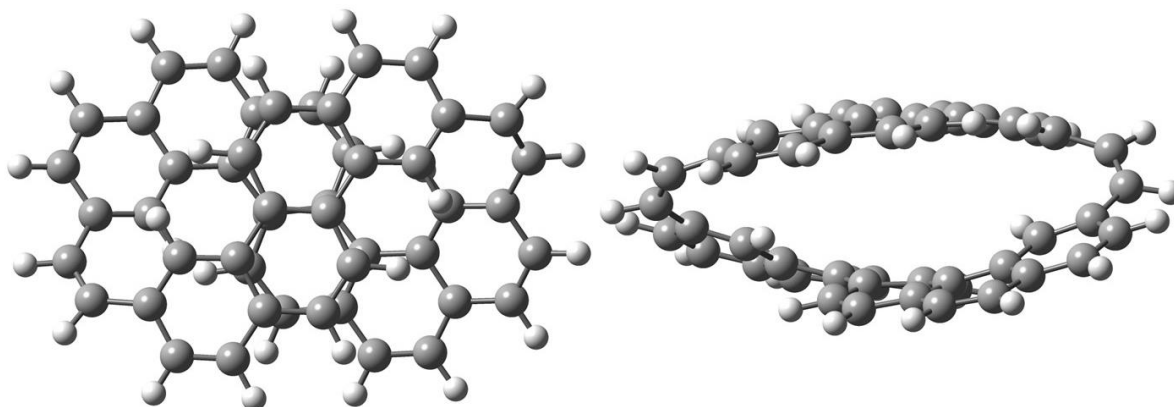


Figure 8. The B3LYP-GD3/6-311+g(d,p) optimized structure of cyclophadien (**R**): top-view (left) and side-view (right).

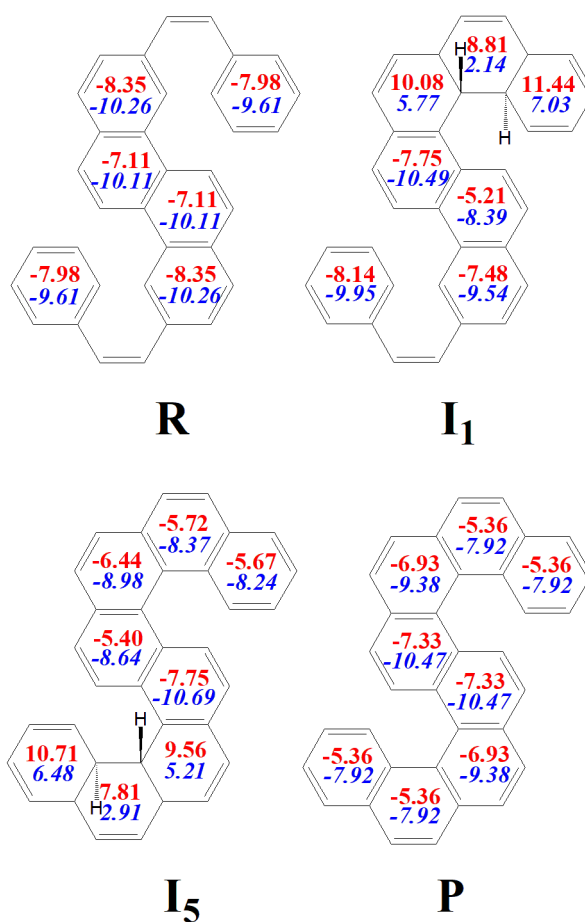


Figure 9. NICS(0) (red numbers) NICS(1)_{av} (blue italic numbers) values for selected compounds involved in the reaction depicted in Figure 7.

Once formed, **I₁** can follow two different reaction pathways. One is a cyclization process on the second reaction center (labeled pathway *a* in Figure 7) and the second is an abstraction of the hydrogen atoms on the reaction center where the cyclization process previously occurred (labeled pathway *b* in Figure 2). Due to the unsymmetrical reaction center, pathway *b* branches further into two different hydrogen abstraction possibilities (intermediates **I_{2b}** and **I_{3b}**) with an insignificant energy difference of 1.79 kcal/mol. The thermodyna-

mically more favorable path is pathway *a*, where cyclization of the second reaction center results in a product **I_{2a}** with the energy of 73.69 kcal/mol relative to the starting cyclophadien **R**. Following that pathway, two possible hydrogen abstractions can occur, now with a more significant energy difference of 4.67 kcal/mol. After this abstraction, the species **I₅** is formed with the energy of 45.21 kcal/mol relative to **R**, which is also the end product of thermodynamically less favorable pathway *b*. Similar to **I₁**, the obtained intermediate **I₅** loses some of its aromaticity since cyclic electron conjugation is disabled in the newly formed hexagon and its neighbor rings.

The intermediate **I₅** undergoes the abstraction to yield two possible intermediates **I₆** and **I₇** whose energies differ insignificantly (0.62 kcal/mol). To gain a final product [12]infinifene, one more abstraction step needs to occur. The final product [12]infinifene is formed with 17.99 kcal/mol relative to the starting reactant **R**. The calculated NICS values revealed that in **1** the aromaticity of all rings which were aromatic in **R** was preserved, and the newly formed rings are also found to be aromatic. Despite a considerable extent of aromaticity in **1**, the reaction is found to be endothermic. This can be explained by a continuous increase of the strain energy as one follows the reaction path from **R** to **1**.

CONCLUSIONS

In this work, we studied the Mallory-type reaction in which the [12]infinifene molecule (**1**) is formed. The electronic structure and aromaticity of chemical species involved in these reactions were studied at the B3LYP-GD3/6-311+g(d,p) level of theory. Also, NICS-Scan and 2D-3D multidimensional magnetic shielding evaluations were carried out at the B3LYP-GIAO/6-311+G(d,p) level of theory. The nonplanarity of **1** was quantified by means of the T index values. It was revealed that **1** is characterized with a substantial extent of cyclic π electron delocalization despite a significant planarity distortion. In agreement, 1D-3D multidimensional magnetic shielding results exhibited magnetic features in [12]infinifene matching those of aromatic molecules. We found that the formation of **1** is an endothermal chemical reaction. The energetics of the examined reaction mechanism showed that there is a tug-of-war between the stabilizing effects of aromaticity and the destabilizing effects of planarity distortions all along the reaction pathway.

Acknowledgments

S.Đ, D.Ć. and S.R. thanks the Ministry of Science, Technological Development and Innovations of the Republic of Serbia (Agreement No. 451-03-47/2023-01/200122). We thank Johannes Endres, TH Nürnberg for technical support, Prof. Tim Clark and Prof. Petra Imhof for hosting this work at the CCC and the Regionales Rechenzentrum Erlangen (RRZE) for a generous allotment of computer time.

References:

- [1] ANJALIKRISHNA, P.K., GADRE, S.R., SURESH, C.H. (2023): Electrostatic potential for exploring electron delocalization in infinifenes, circulenes, and nanobelts. *Journal of Organic Chemistry* **88**: 4123–4133. doi: 10.1021/acs.joc.2c02507
- [2] ANTHONY, J.E. (2006): Functionalized acenes and heteroacenes for organic electronics. *Chemical Reviews* **106** (12): 5028–5048. doi: 10.1021/cr050966z.

- [3] BECKE, A.D. (1993): Density-functional Thermochemistry. III. The role of exact exchange. *The Journal of Chemical Physics* **98** (7): 5648–5652. doi: 10.1063/1.464913.
- [4] BENDIKOV, M., WUDL, F., PEREPICHKA, D.F. (2004): Tetrathiafulvalenes, Oligoacenes, and their buckminsterfullerene derivatives: the brick and mortar of organic electronics. *Chemical Reviews* **104** (11): 4891–4946. doi: 10.1021/cr030666m.
- [5] CHEN, Z., WANNERE, C.S., CORMINBOEUF, C., PUCHTA, R., SCHLEYER, P. VON R. (2005): Nucleus-independent chemical shifts (nics) as an aromaticity criterion. *Chemical Reviews* **105** (10): 3842–3888. doi: 10.1021/cr030088+.
- [6] DOBROWOLSKI, J. Cz., LIPIŃSKI, P.F.J. (2016): On splitting of the nics(1) magnetic aromaticity index. *RSC Advances* **6** (28): 23900–23904. doi: 10.1039/C6RA03246J.
- [7] FEIXAS, F., MATITO, E., POATER, J., SOLÀ, M. (2007): Aromaticity of distorted benzene rings: exploring the validity of different indicators of aromaticity. *The Journal of Physical Chemistry A* **111** (20): 4513–4521. doi: 10.1021/jp0703206.
- [8] FRISCH, M.J., TRUCKS, G.W., SCHLEGEL, H.B., SCUSERIA, G.E., ROBB, M.A., CHEESEMAN, J.R., SCALMANI, G., BARONE, V., MENNUCCI, B., PETERSSON, G.A., NAKATSUJI, H., CARICATO, M., LI X., HRATCHIAN, H.P., IZMAYLOV, A.F., BLOINO, J., ZHENG, G., SONNENBERG, J.L., HADA, M., EHARA, M., TOYOTA, K., FUKUDA, R., HASEGAWA, J., ISHIDA, M., NAKAJIMA, T., HONDA, Y., KITAO, O., NAKAI, H., VREVEN, T., MONTGOMERY, J.A., PERALTA, J.E., OGLIARO, F., BEARPARK, M., HEYD, J.J., BROTHERS, E., KUDIN, K.N., STAROVEROV, V.N., KOBAYASHI, R., NORMAND, J., RAGHAVACHARI, K., RENDELL, A., BURANT, J.C., IYENGAR, S.S., TOMASI, J., COSSI, M., REGA, N., MILLAM, J.M., KLENE, M., KNOX, J.E., CROSS, J.B., BAKKEN, V., ADAMO, C., JARAMILLO, J., GOMPERS, R., STRATMANN, R.E., YAZYEV, O., AUSTIN, A.J., CAMMI, R., POMELLI, C., J. OCHTERSKI, W., MARTIN, R. L., MOROKUMA, K., ZAKRZEWSKI, V.G., VOTH, G.A., SALVADOR, P., DANNENBERG, J.J., DAPPRICH, S., DANIELS, A.D., FARKAS, FORESMAN, J.B., ORTIZ, J.V., CIOSLOWSKI, J., FOX, D.J. (2010): Gaussian 09, Revision C.01.
- [9] GERSHONI-PORANNE, R., STANGER, A. (2015): Magnetic criteria of aromaticity. *Chemical Society Reviews* **44** (18): 6597–6615. doi: 10.1039/C5CS00114E.
- [10] GRIMME, S., ANTONY, J., EHRlich, S., KRIEG, H. (2010): A consistent and accurate ab initio parametrization of density functional dispersion correction (dft-d) for the 94 elements h-pu. *The Journal of Chemical Physics* **132** (15): 154104. doi: 10.1063/1.3382344.
- [11] GUTMAN, I., JANOŠEVIĆ, M., RADENKOVIĆ, S. (2011): Effect of benzocyclobutadieno-annulation on cyclic conjugation in coronene. *Kragujevac Journal of Science* **33**: 45–53.
- [12] HOU, H., ZHAO, X-J., TANG, C., JU, Y-Y., DENG, Z-Y., WANG, X-R., FENG, L-B., LIN, D-H., HOU, X., NARITA, A., MÜLLEN, K., TAN, Y-Z. (2020): Synthesis and assembly of extended quintulene. *Nature Communications* **11** (1): 3976. doi: 10.1038/s41467-020-17691-7.
- [13] JØRGENSEN, K.B. (2010): Photochemical oxidative cyclisation of stilbenes and stilbenoids—the mallory-reaction. *Molecules* **15** (6): 4334–4358.
- [14] KRYGOWSKI, T.M., SZATYLOWICZ, H., STASYUK, O.A., DOMINIKOWSKA, J., PALUSIAK, M. (2014): Aromaticity from the viewpoint of molecular geometry: application to planar systems. *Chemical Reviews* **114** (12): 6383–6422. doi: 10.1021/cr400252h.
- [15] KRZESZEWSKI, M., ITO, H., ITAMI, K. (2022): Infinitene: a helically twisted figure-eight [12]circulene topoisomer. *Journal of the American Chemical Society* **144** (2): 862–871. doi: 10.1021/jacs.1c10807.

- [16] LEE, C., YANG, W., PARR, R.G. (1988): Development of the colle-salvetti correlation-energy formula into a functional of the electron density. *Physical Review B* **37** (2): 785–789. doi: 10.1103/PhysRevB.37.785.
- [17] MILLER, R.W., DUNCAN, A.K., SCHNEEBELI, S.T., GRAY, D.L., WHALLEY, A.C. (2014): Synthesis and structural data of tetrabenzo[8]circulene. *Chemistry – A European Journal* **20** (13): 3705–3711. doi: 10.1002/chem.201304657.
- [18] MONACO, G., ZANASI, R., SUMMA, F.F. (2022): Magnetic characterization of the infinitene molecule. *The Journal of Physical Chemistry A* **126** (23): 3717–3723. doi: 10.1021/acs.jpca.2c02339.
- [19] NARITA, A., WANG, X-Y., FENG, X., MÜLLEN, K. (2015): New advances in nanographene chemistry. *Chemical Society Reviews* **44** (18): 6616–6643. doi: 10.1039/C5CS00183H.
- [20] NAULET, G., STURM, L., ROBERT, A., DECHAMBENOIT, P., RÖHRICHT, F., HERGES, R., BOCK, H., DUROLA, F. (2018): Cyclic tris-[5]helicenes with single and triple twisted möbius topologies and möbius aromaticity. *Chemical Science* **9** (48): 8930–8936. doi: 10.1039/C8SC02877J.
- [21] NOVOSELOV, K.S., GEIM, A.K., MOROZOV, S.V., JIANG, D., ZHANG, Y., DUBONOS, S.V., GRIGORIEVA, I.V., FIRSOV, A.A. (2004): Electric field effect in atomically thin carbon films. *Science* **306** (5696): 666–669. doi: 10.1126/science.1102896.
- [22] OROZCO-IC, M., VALIEV, R.R., SUNDHOLM, D. (2022): Non-intersecting ring currents in [12]infinitene. *Physical Chemistry Chemical Physics* **24** (11): 6404–6409. doi: 10.1039/D2CP00637E.
- [23] OTERO-LOBATO, M.J., KAATS-RICHTERS, V.E. M., KOPER, C., VLIETSTRA, E.J., HAVENITH, R.W.A., JENNESKENS, L.W., SEINEN, W. (2005): CP-arene oxides: the ultimate, active mutagenic forms of cyclopenta-fused polycyclic aromatic hydrocarbons (CP-PAHs). *Mutation Research/Genetic Toxicology and Environmental Mutagenesis* **581** (1): 115–132. doi: 10.1016/j.mrgentox.2004.11.014
- [24] PUCHTA, R., ĐORĐEVIĆ, S., RADENKOVIĆ, S., JIAO, H., VAN EIKEMA HOMMES, N.J.R. (2022): 25 years of nics – much more than nothing! *Journal of the Serbian Chemical Society* **87** (12): 1439–1446. doi: 10.2298/JSC211203057P.
- [25] RANDIĆ, M. (2003): Aromaticity of polycyclic conjugated hydrocarbons. *Chemical Reviews* **103** (9): 3449–3606. doi: 10.1021/cr9903656.
- [26] REDŽEPOVIĆ, I., MARKOVIĆ, S., TOŠOVIĆ, J. (2017): Antioxidative activity of caffeic acid – mechanistic DFT study. *Kragujevac Journal of Science* **39**: 109–122. doi: 10.5937/KgJSci1739109R.
- [27] REDŽEPOVIĆ, I., MARKOVIĆ, S., FURTULA B. (2019): On structural dependence of enthalpy of formation of catacondensed benzenoid hydrocarbons. *MATCH Communications in Mathematical and in Computer Chemistry* **82**: 663–678.
- [28] SCHLEYER, P. VON R., MAERKER, C., DRANSFELD, A., JIAO, H., VAN EIKEMA HOMMES, N.J.R. (1996): Nucleus-independent chemical shifts: a simple and efficient aromaticity probe. *Journal of the American Chemical Society* **118** (26): 6317–6318. doi: 10.1021/ja960582d.
- [29] SCHLEYER, P. VON R., JIAO, H., VAN EIKEMA HOMMES, N.J.R., MALKIN, V.G., MALKINA O.L. (1997): An evaluation of the aromaticity of inorganic rings: refined evidence from magnetic properties. *Journal of the American Chemical Society* **119** (51): 12669–12670.

doi: 10.1021/ja9719135.

- [30] STANGER, A. (2006): Nucleus-independent chemical shifts (nics): distance dependence and revised criteria for aromaticity and antiaromaticity. *The Journal of Organic Chemistry* **71** (3): 883–893. doi: 10.1021/jo051746o.
- [31] STEPHENS, P.J., DEVLIN, F.J., CHABALOWSKI, C.F., FRISCH, M.J. (1994): Ab initio calculation of vibrational absorption and circular dichroism spectra using density functional force fields. *The Journal of Physical Chemistry* **98** (45): 11623–11627. doi: 10.1021/j100096a001.
- [32] TOŠOVIĆ, J. (2017): Spectroscopic features of caffeic acid: theoretical study. *Kragujevac Journal of Science* **39**: 99-108. doi: 10.5937/KgJSci1739099T.
- [33] WEISMAN, J.L., LEE, T.J., SALAMA, F., HEAD-GORDON, M. (2003): Time-dependent density functional theory calculations of large compact polycyclic aromatic hydrocarbon cations: implications for the diffuse interstellar bands. *The Astrophysical Journal* **587** (1): 256. doi: 10.1086/368103.
- [34] XIA, Z., PUN, S.H., CHEN, H., MIAO, Q. (2021): Synthesis of zigzag carbon nanobelts through scholl reactions. *Angewandte Chemie International Edition* **60** (18): 10311–10318. doi: 10.1002/anie.202100343.